



**Self-assembly fabrication of graphene/multi-walled carbon nanotube hybrid material for suppressing potential heat radiation and toxic effluent of polymer**

|                               |  |
|-------------------------------|--|
| Journal:                      | <i>RSC Advances</i>  |
| Manuscript ID                 | RA-ART-09-2015-019227.R1   |
| Article Type:                 | Paper  |
| Date Submitted by the Author: | 13-Nov-2015  |
| Complete List of Authors:     | Liu, Lei; Southeast University, School of Mechanical Engineering<br>Wang, Dong; University of Science and Technology of China, State Key Lab of Fire Science<br>Hu, Yuan; University of Science and Technology of China, State Key Lab of Fire Science |
| Subject area & keyword:       | Carbon materials < Materials   |
|                               |  |

**Self-assembly fabrication of graphene/multi-walled carbon  
nanotube hybrid material for suppressing potential heat  
radiation and toxic effluent of polymer**

Lei Liu,<sup>\*,†</sup> Dong Wang,<sup>‡</sup> Yuan Hu,<sup>\*,‡</sup>

<sup>†</sup> School of Mechanical Engineering, Southeast University, Nanjing 210096,  
People's Republic of China

<sup>‡</sup> State Key Laboratory of Fire Science, University of Science and Technology of  
China, 96 Jinzhai Road, Hefei, Anhui 230026, P. R. China

**Corresponding Author**

\*Tel./Fax: +86-25-52090501. E-mail: liulei@seu.edu.cn.

\*Tel./Fax: +86-551-63601664. E-mail: yuanhu@ustc.edu.cn.

**Abstract:**

In the study, negative graphene oxide were combined with positive chitosan-modified multi-walled carbon nanotube in aqueous solution and then thermally reduced to fabricate multi-walled carbon nanotube/graphene (MWCNT/G) hybrid material. The hybrid material solved the aggregation of graphene during thermal reduction, which was contributed to the dispersion of graphene in polymer matrix. It displayed outstanding properties in suppressing heat radiation and toxic effluent that were superior to either MWCNT or graphene alone. After incorporating the hybrid into epoxy matrix, the peak heat release rate and total heat release of MWCNT/G/EP nanocomposites were decrease by 34.9% and 25.0% compared to neat epoxy. And the hybrid dramatically decreased toxic effluent including hydrocarbons, CO and aromatic compounds. Finally, the possible mechanisms of suppressing heat radiation and toxic effluent were reasonably proposed.

## 1. Introduction

Epoxy resin (EP) is a thermosetting polymer material, which is widely applied in various industries such as coating, adhesive, electrical insulation, and composite applications.<sup>1-4</sup> Nevertheless, intrinsic flammability is one of the main drawbacks, vastly limiting its application.<sup>5,6</sup> The burning EP would produce the heat radiation and toxic effluent, possibly causing death or permanent injury in fire accident.<sup>7, 8</sup> Therefore, efficient suppression of heat radiation and toxic effluent released during combustion will save lives and health injuries in real fires.

Graphene, an emerging member of carbon-based materials, has exhibited excellent performance in flame retardance of polymer-based composites, because of its unique two-dimensional (2D)  $sp^2$ -hybridized carbon sheet with large surface to act as an effective barrier to suppress heat and pyrolysis products.<sup>9-11</sup> Whereas, graphene usually tend to restack, owing to the strong  $\pi$ - $\pi$  interaction among nanosheets.<sup>12, 13</sup> Thus, graphene nanosheets are easily aggregated in polymer matrix, weakening the ability to suppress heat radiation and toxic effluent.

As one of the most promising carbon-based materials, carbon nanotube (CNT), has attracted considerable interest in polymer composites, due to its uniquely excellent properties with high aspect ratio.<sup>14-16</sup> In recent years, researchers have focused on the study of CNT to suppress heat radiation and toxic effluent. Kashiwagi *et al.* have demonstrated that CNTs resulted in a significant reduction in heat release rate (HRR) of polymer materials, which was attributed to the formation of a continuous network-structured protective layer consisted of CNTs to act as a heat

shield for the virgin polymer below the layer.<sup>17</sup> In addition, the protective network composed of CNTs could prevent the escape of toxic effluent such as CO, hydrocarbon, aromatic compounds and absorb the oxygen molecules.<sup>18</sup> The compactness of CNT network depends on the dispersion of CNTs in polymer matrix, which determines the suppressive efficiency.<sup>17</sup> Unfortunately, the entanglement of CNTs deteriorates their dispersion level.<sup>19,20</sup>

Based on the above, the positive chitosan-modified MWCNTs were inserted onto negative graphene oxide (GO) to fabricate MWCNT/GO hybrid material in aqueous solution via a self-assembly method and then it was thermally reduced to MWCNT/G hybrid material, solving the aggregation of graphene nanosheets and the entanglement of MWCNTs. And MWCNT/G hybrid material was incorporated into epoxy matrix to suppress potential heat radiation and toxic effluent during combustion.

## **2. Experimental section**

### **2.1 Materials**

Graphite powder, concentrated sulfuric acid (98%), sodium nitrate, potassium permanganate, 30% H<sub>2</sub>O<sub>2</sub> solution, acetic acid, hydrochloric acid and CS (viscosity: 50-800 mPa·s, degree of deacetylation: 80-95%), tetrahydrofuran (THF) and 4,4'-aminodiphenylmethane (DDM) were purchased from Sinopharm Chemical Reagent Co., Ltd. (China). EP resin (E-51) with an epoxy value of 0.51 mol/100 g was obtained from Hefei Jiangfeng chemical industry Co., Ltd (China).

## 2.2 Synthesis of MWCNT/G hybrid material

GO was prepared from graphite powder by a modified Hummers method.<sup>21</sup> The synthetic process of MWCNT/G hybrids was shown in Scheme 1a. CS was dissolved in acetic acid aqueous solution (1 wt%) with mechanical stirring for 12 h at room temperature to obtain a 0.05 wt% homogeneous solution. Subsequently, a certain amount of MWCNTs were dispersed in CS solution. The dispersion process was conducted at room temperature with the assistance of sonication for 48 h. Then, the aqueous solution of GO with the same quality to MWCNT was added into the dispersion above and ultrasonicated for 8 h to get MWCNT/GO hybrid material. The resulting product was separated by filtration, washed with deionized water and dried at 60 °C under vacuum overnight. Afterwards, the hybrid were heated at 800 °C in nitrogen atmosphere for 4 h to obtain MWCNT/G hybrid material. Similarly, MWCNT/2G hybrid was prepared by the same synthetic route except the addition of double portion of GO.

## 2.3 Preparation of EP composites

EP composites were prepared via the solution blending method, holding the nanofiller loading at 2 wt%. In brief, the preparation of EP composites was performed as follows: nanofillers were added into THF with microthermal sonication for 20 min to form a black suspension. Then EP oligomers were added into the suspension above and mechanically stirred for 12 h until homogeneous mixtures were obtained. Afterwards, the mixtures were heated to remove the solvent. Later, DDM was melted at 150 °C

and then added into the mixtures at 100 °C. The mixture was stirred for 5 min, poured into a Teflon mold, pre-cured in an oven at 100 °C for 2 h and post-cured at 150 °C for another 2 h.

#### **2.4 Characterization**

Transmission electron microscopy (TEM) (JEM-2100F, Japan Electron Optics Laboratory Co., Ltd., Japan) was utilized to inspect the microstructure of the nanomaterials and the ultrathin section morphology of EP composite. The accelerating voltage was 200 kV.

Fourier transform infrared (FT-IR) spectra were obtained from a Nicolet 6700 spectrometer (Nicolet Instrument Co., US). The samples were mixed with KBr powders and pressed into tablets for characterization.

Thermogravimetric analysis (TGA) was implemented with the aid of a Q5000 IR thermal analyzer (TA Instruments Inc., US) in the range between indoor temperature and 800 °C. The heating rate is 20 °C/min.

The specimens of EP composites were cryogenically fractured in liquid nitrogen first and then sputter-coated with a conductive layer. The morphology of the fractured samples was studied by a PHILIPS XL30E scanning electron microscope (SEM, FEI Co., Ltd., U.S.).

The flame retardance of the samples were performed on micro combustion calorimeter (MCC, Govmark Organization, Inc., Farmingdale, NY) according to ASTM D 7309-07 and a cone calorimeter (Fire Testing Technology, U.K.) on the basis of ISO 5660.

Thermogravimetric analysis/infrared spectrometry (TG-IR) of the samples was performed using a TGA Q5000 IR thermogravimetric analyzer that was interfaced to a Nicolet 6700 FT-IR spectrophotometer.

### 3. Results and discussion

#### 3.1 Characterization of MWCNT/G hybrids

The morphology of G, MWCNT/2G and MWCNT/G hybrids were investigated by TEM and SEM (Fig. 1). Graphene shows a typically flat yet seriously folded nanoplatelet with a few hundred nanometers. MWCNT/2G and MWCNT/G hybrids exhibit lamellar graphene nanosheets and separated MWCNTs. Besides, SEM image of MWCNT/G hybrids reveals the successful decoration of MWCNTs onto graphene nanosheets.

The FT-IR spectra of CS, GO, MWCNT, G, CS-MWCNT, MWCNT/2G and MWCNT/G hybrids are shown in Fig. 2. CS has two characteristic bands located at 1656 and 1598  $\text{cm}^{-1}$ , which are ascribed to the C=O stretching vibration of -NHC(O)- and the N-H bending mode of -NH<sub>2</sub>, respectively. Compared to pure MWCNT, CS-MWCNT shows a new strong absorption peak at 1582  $\text{cm}^{-1}$  related to N-H bending emerges and the band at 1630  $\text{cm}^{-1}$  disappears, possibly because CS are absorbed onto MWCNT. GO has one absorption band at 1724  $\text{cm}^{-1}$  from carbonyl and carboxylic groups. Compared with GO, the peak at 1724  $\text{cm}^{-1}$  disappears in the spectra of graphene, due to the thermal reduction of carbonyl and carboxylic groups of GO, and the new peak at 1630  $\text{cm}^{-1}$  is ascribed to C=C groups. In the spectra of

MWCNT/G and MWCNT/2G hybrids, the peak at  $1630\text{ cm}^{-1}$  appears again, because of the thermal reduction of oxygen-containing groups and thermal decomposition of chitosan.

Herein, the influence of MWCNTs on the thermal stability of graphene was investigated by TGA. Fig. 3 shows TGA curves of MWCNT, G, MWCNT/2G and MWCNT/G hybrids recorded under air atmosphere. The pyrolysis process of G and MWCNT consists of deoxygenation and subsequent oxidation of the char. In comparison, MWCNT/2G and MWCNT/G hybrids display a similar thermogravimetric profile to graphene. Whereas, the residue percentage of MWNT/G hybrids is much higher than MWCNT/2G and G, indicating appropriate MWCNTs could improve the thermal oxidative resistance of graphene.

### **3.2 Microstructure of the fractured surface of EP composites**

Dispersion states of the nanofillers in the matrix was directly observed in the SEM images of fractured surface of EP composites (Fig. S1, Supporting Information). Serious entanglement and agglomeration of MWCNTs appears in SEM images of MWCNT/EP composites (Fig. S1 c and d, Supporting Information). Nevertheless, individual MWCNTs are uniformly distributed in MWCNT/2G/EP and MWCNT/G/EP composites, indicating the immobilization of MWCNTs onto graphene nanosheets prevents the entanglement and agglomeration of MWCNTs during the preparation process of EP composites. In addition, several graphene agglomerates are pulled out from the matrix in Fig S1 e and f (Supporting

Information), while none is dragged out of EP matrix, suggesting surface immobilized MWNTs inhibits the agglomeration of graphene nanosheets.

To further investigate the dispersion state of MWCNTs and graphene nanosheets in MWCNT/G/EP composite, the ultrathin section of the composite was observed by TEM. Fig. S2 (Supporting Information) shows that many individual MWCNTs homogeneously disperse in epoxy matrix. Moreover, only a few graphene nanosheets are obscure, demonstrating no obvious aggregation of graphene exists.

### 3.3 Thermal stability of EP and its composites

The whole combustion behavior of polymer materials consists of the combustion behavior of surface materials and the pyrolysis behavior of underlying materials simultaneously. The pyrolysis behavior of underlying materials is usually investigated by TGA. TGA and DTG curves of EP and its composites are presented in Fig. 4. On the basis of DTG curves, it can be seen that the thermal degradation process of EP and its composites could be divided into the decomposition of polymeric networks and thermal oxidation of the generated char. In order to study the thermal stability of the samples, their degradation temperatures are usually compared with each other. The typical degradation temperatures are the onset degradation temperatures termed as  $T_{\text{onset}}$ , the temperature at the maximum decomposition rate of polymeric networks called as  $T_{\text{max1}}$ , and the temperature at the maximum thermal oxidation rate of the generated char named as  $T_{\text{max2}}$ .  $T_{\text{onset}}$ s of EP composites, defined as the temperatures at which the mass loss is 5%, are lower than pure EP. This can be explained that good

thermal conductivity of MWCNT and/or graphene can speed up the diffusion of heat in EP matrix to accelerate pyrolysis of composites.  $T_{\max 1S}$  of EP composites are very close to neat EP, interpreted by the combination of the physical barriers of MWCNTs and/or graphene nanosheets to retard the release of decomposition volatiles and high thermal conductivity to facilitate the polymer pyrolysis. In the case of  $T_{\max 2S}$  of EP composites, they are increased compared to pure EP, because the physical barriers of MWCNTs and/or graphene nanosheets prevent the permeation of oxygen to delay char oxidation. Also, physical barriers of MWCNTs and/or graphene nanosheets should be responsible for lower maximum decomposition rates and more char residue of EP composites. MWCNT/G/EP composites exhibit the lowest maximum decomposition rate and the maximum char residue.

### **3.4 Heat radiation of burning EP and its composites**

The flame-retardant performance of EP and its composites was measured via the MCC which is a reliable small-scale measurement instrument to investigate the peak heat release rate (PHRR) of materials.<sup>22</sup> PHRR is one of the most important indicators that evaluate the combustion properties of materials. Fig. 5 shows the HRR curves of pure EP and its composites. When MWCNTs or graphene nanosheets are incorporated into EP matrix, the PHRR values are decreased from 310 W/g to 280 and 224 W/g, nearly 9.7% and 29.0% reduction compared to pure EP. Interestingly, the PHRR value of MWCNT/2G/EP composites is nearly the same as G/EP. Furthermore, MWCNT/G/EP composites have the lowest PHRR, indicating the lowest heat radiation during combustion.

So as to accurately estimate heat radiation of polymer materials, cone calorimeter is the most commonly used tools under the real fire scene.<sup>23</sup> PHRR, peak smoke production rate (PSPR), total heat release (THR), time to ignition (TTI) and fire growth index (FGI) obtained from the cone test are all important parameters for indicating fire hazards of materials. PHRR and PSPR are two important parameters to study the heat radiation, respectively. The HRR and THR profiles of EP and its composites are shown in Fig. 6 and the corresponding data are recorded in Table 1 as well. PHRR of pure EP reaches up to  $1592 \text{ kW/m}^2$ , indicating that the combustion of EP would liberate a large amount of heat. Compared to pure EP, the addition of 2 wt% MWCNTs or graphene nanosheets results in the PHRR of EP matrix decrease to 1490 and  $1237 \text{ kW/m}^2$ , respectively. In the case of MWCNT/2G/EP composite, the PHRR is also reduced to  $1289 \text{ kW/m}^2$ , approximately 19.0% reduction in comparison with pure EP. Furthermore, MWNT/G/EP composite shows more significant decrease in PHRR, corresponding to 34.9% reduction. Generally, THR is related to the burning degree of materials. The THR values of MWNT/EP, G/EP, MWNT/2G/EP and MWNT/GNS/EP composites decrease in a certain content, amounting to 2.7%, 12.8%, 13.5% and 25.0% reduction successively, in comparison to pure epoxy. The decline in THR demonstrates that some EP chains participated in the carbonization process.

It is well known that carbon-based compounds are liberated from flaming polymer and aggregated to yield smoke particles, lowering the visibility of fire scene. From Table 1, PSPR values of MWCNT/EP, GNS/EP, MWCNT/2G/EP and MWCNT/G/EP composites are lessened by 10.8%, 20.9%, 44.7% and 56.7% in

sequence, compared to pure EP resin. When polymer sample is heated to generate volatile combustible products, it would be ignited until the concentration of volatile gas is dense enough. TTIs of epoxy composites are longer than pure EP, because graphene nanosheets and/or MWCNTs block the release of volatile gas. The prolonged TTI declares the elevated fire safety.

FGI, defined as the ratio of PHRR and time to PHRR, is an overall index to evaluate the fire hazards of materials.<sup>24</sup> The lower FGI of materials, the lower fire hazards. The lowest FGI value of MWCNT/G/EP composites demonstrates the highest fire safety of the material.

### 3.5 Toxic effluent

According to previous reports, it is informed that the analysis of toxic effluent released from pyrolysis would contribute to study thermal degradation process and non-thermal hazards.<sup>25</sup> The pyrolysis products are usually monitored and analyzed by TG-IR technique which can identify exactly gaseous category via the position of specific peak and determine semiquantitatively gaseous amount by the intensity of the characteristic peak. Fig. S3 (Supporting Information) presents FT-IR spectra of gaseous products of neat EP and MWCNT/G/EP composite at different stages of pyrolysis process. Hydrocarbons ( $3100\text{-}2800\text{ cm}^{-1}$ ),  $\text{CO}_2$  ( $2360\text{ cm}^{-1}$ ),  $\text{CO}$  ( $2180\text{ cm}^{-1}$ ) and aromatic compounds ( $1605$ ,  $1510$  and  $1460\text{ cm}^{-1}$ ) escaped from EP matrix are distinctly characterized in the spectra. The same peaks of the pyrolysis products exist in the spectra of both EP and MWCNT/G/EP, indicating that MWCNT/G hybrid has little impact on decomposition mode of EP chains. As can be observed, the

characteristic peaks of aromatic compounds emerge in the spectrum of MWCNT/G/EP composites at 300 °C, yet they are absent from that of neat EP, probably because thermal conductivity of the well-dispersed MWCNTs and graphene nanosheets in the EP matrix promotes thermal degradation of the materials.

To compare toxic effluent of EP and MWNT/G/EP composite, the intensity of the pyrolysis products is shown in Fig. 7. Fig. 7a shows the comparison of total gas volatiles for EP and MWCNT/G/EP composite. The absorbance of total gas volatiles for MWCNT/G/EP composites is much lower than that for neat EP, meaning better overall smoke safety of MWCNT/G/EP composite. Hydrocarbons and aromatic compounds are the main organic volatiles, which may be self-assembled to smoke particles for reducing visibility and increasing poisonous to human health. In the case of MWCNT/G/EP composites, the absorbance of hydrocarbons and aromatic compounds are obviously dropped by 37.4% and 40.0%, respectively. In terms of toxicity, CO is the main killer to human trapped in a fire. As expected, CO yield for MWCNT/G/EP composite is much lower than neat EP, probably ascribed to the CO has been hindered by MWCNTs and graphene nanosheets, and oxidized by oxygen absorbed onto MWCNTs and graphene nanosheets. In short, the reduction in hydrocarbons, aromatic compounds and CO for MWCNT/G/EP composites would be favorable for fire rescue, when a fire accident occurs.

### **3.7 Analysis of char residues**

Generally, the analysis of char residues after combustion contributes to the investigation of flame retardant mechanism. Digital photos of the char residues reflect

the macroscopic morphologies, and SEM images of exterior chars reveal the microcosmic structure. The digital photos of residual chars after cone tests are shown in Fig. S4 (Supporting Information). As can be seen, little and scattered char residues of neat EP are left in the an aluminum foil. When MWCNTs or graphene nanosheets alone are incorporated into the matrix, the amount of char residues is increased, but still scattered in the test box. In the case of MWCNT/2G/EP composite, char residues increase and cover most of the test box. As for MWCNT/G/EP composite, the char residues are the maximum and completely cover the whole aluminum foil.

As shown in Fig. 8, char layer of neat EP exhibits a loose and multi-porous structure, while MWCNT/EP presents a multi-porous but firm surface with many cracks, and G/EP shows a multi-porous and firm appearance with no cracks. In addition, there are a few cracks on the char surface of MWCNT/2G/EP composites, but no holes and cracks in char layer of MWCNT/G/EP composites, which is attributed to the mechanism that the addition of the well- dispersed MWCNTs and graphene nanosheets improves the strength of the char layer so that the gaseous products cannot break the exterior chars, leaving a smooth and compact surface. It is common knowledge that the more compact char layer results in more effective insulation to heat and volatiles.

### **3.8 The mechanism of suppressing heat radiation and toxic effluent**

In general, the suppression of heat radiation and toxic effluent of EP composites are superior to neat epoxy, and MWCNT/G/EP composites show the most excellent

performance. Based on the analysis of heat radiation and toxic effluent during combustion, it is speculated that the formation of multi-layered barrier networks composed of MWCNTs and/or graphene nanosheets in epoxy matrix would not only prevent the permeation of heat and oxygen into the underlying matrix during combustion, but also inhibit the effusion of heat radiation and toxic effluent. Meanwhile, the different degree of suppressing heat radiation and toxic effluent of EP composites depend on the continuity, compactness and thermal resistance of barrier networks, which is vividly depicted in Fig. 9. The more continuous, compact and thermally stable barrier networks result in the higher suppression of heat radiation and toxic effluent. Due to unique 2D structure of graphene, barrier networks composed of graphene nanosheets are more compact than MWCNTs, therefore graphene nanosheets show better heat and gas insulation, resulting in higher suppression of G/EP than MWCNT/EP composites. Interestingly, it is observed that the suppression of heat radiation and toxic effluent of MWCNT/2G/EP composites is more or less similar to that of G/EP, indicating the reduction in aggregation of graphene nanosheets caused by the intercalation of MWCNTs has little effect on the continuity and compactness of barrier networks. However, MWCNT/G/EP composite shows more higher suppression of than MWCNT/2G/EP, probably because moderate level of MWCNTs will promote the dispersion of graphene nanosheets in EP matrix, and tremendously improves the compactness of barrier networks. Moreover, sufficient MWCNTs onto graphene protect heat invasion, thus enhancing thermally stability of barrier networks, and MWCNTs act as bridges for the isolated GNSs, thus increasing

the continuity of barrier networks.

#### **4. Conclusions**

In this paper, MWCNT/G hybrid material was prepared with a self-assembly method, confirmed by TEM, SEM, FT-IR and Raman spectroscopy. TGA results revealed that functionalization with adequate MWCNTs could improve thermal resistance of graphene. SEM and TEM images of MWCNT/G/EP composite indicated that plenty of separated MWCNTs and exfoliated graphene nanosheets are well-dispersed in epoxy matrix. The incorporation of MWCNTs and/or graphene nanosheets into EP matrix led to lower maximum decomposition rate compared to neat EP. PHRR and THR values of MWCNT/G/EP composite were decreased by 34.9% and 25.0%, respectively, compared with pure EP. TG-IR results demonstrated that toxic volatiles including hydrocarbons, CO and aromatic compounds of MWCNT/G/EP composites are significantly lessened in MWCNT/G/EP composite. Finally, the barrier networks formed by MWCNTs and graphene nanosheets were reasonably proposed to explain the possible mechanism of suppressing heat radiation and toxic effluent of EP composites.

#### **Acknowledgements**

The work was financially supported by the National Natural Science Foundation of China (U1332134) and National Natural Science Foundation of China (NO. 21374111).

**References :**

1. K. Kowalczyk and T. Spychaj, *Surf. Coat. Tech.*, 2009, **204**, 635-641.
2. H. Jin, G. M. Miller, N. R. Sottos and S. R. White, *Polymer*, 2011, **52**, 1628-1634.
3. O. Eksik, J. Gao, S. A. Shojaei, A. Thomas, P. Chow, S. F. Bartolucci, D. A. Lucca and N. Koratkar, *ACS nano*, 2014, **8**, 5282-5289.
4. X. Wang, J. Jin and M. Song, *Carbon*, 2013, **65**, 324-333.
5. D. Wang, K. Zhou, W. Yang, W. Xing, Y. Hu and X. Gong, *Ind. Eng. Chem. Res.*, 2013, **52**, 17882-17890.
6. J. Jiang, Y. Cheng, Y. Liu, Q. Wang, Y. He and B. Wang, *J. Mater. Chem. A*, 2015, **3**, 4284-4290.
7. S. D. Jiang, Z. M. Bai, G. Tang, L. Song, A. A. Stec, T. R. Hull, Y. Hu and W. Z. Hu, *ACS Appl. Mater. Interfaces*, 2014, **6**, 14076-14086.
8. S.-D. Jiang, Z.-M. Bai, G. Tang, Y. Hu and L. Song, *Ind. Eng. Chem. Res.*, 2014, **53**, 6708-6717.
9. S.-D. Jiang, Z.-M. Bai, G. Tang, Y. Hu and L. Song, *Compos. Sci. Technol.*, 2014, **102**, 51-58.
10. S. Liu, H. Yan, Z. Fang and H. Wang, *Compos. Sci. Technol.*, 2014, **90**, 40-47.
11. X. Wang, W. Xing, X. Feng, B. Yu, L. Song and Y. Hu, *Polym. Chem.*, 2014, **5**, 1145-1154.
12. J. Sarabadani, A. Naji, R. Asgari and R. Podgornik, *Phys. Rev. B.*, 2011, **84**.
13. G. Gómez-Santos, *Phys. Rev. B.*, 2009, **80**.
14. S. Kim, F. Fornasiero, H. G. Park, J. B. In, E. Meshot, G. Giraldo, M. Stadermann, M. Fireman, J. Shan, C. P. Grigoropoulos and O. Bakajin, *J. Membrane. SCI.*, 2014, **460**, 91-98.

- 15.M. H. Al-Saleh and U. Sundararaj, *Carbon*, 2009, **47**, 1738-1746.
- 16.T. Kashiwagi, , Eric Grulke, Jenny Hilding, Richard Harris and J. D. Walid Awad, *Macromol. Rapid. Commun.*, 2002, **23**, 761-765.
- 17.T. Kashiwagi, F. Du, J. F. Douglas, K. I. Winey, R. H. Harris, Jr. and J. R. Shields, *Nat. Mater.*, 2005, **4**, 928-933.
- 18.Q. Zhang, J. Zhan, K. Zhou, H. Lu, W. Zeng, A. A. Stec, T. R. Hull, Y. Hu and Z. Gui, *Polym. Degrad. Stabil.*, 2015, **115**, 38-44.
- 19.P.-C. Ma, N. A. Siddiqui, G. Marom and J.-K. Kim, *Compos Part A: Appl Sci Manufac.*, 2010, **41**, 1345-1367.
- 20.Y. Liu, J. Tang, X. Chen and J. H. Xin, *Carbon*, 2005, **43**, 3178-3180.
- 21.W. S. Hummers and R. E. Offeman, *J. Am. Chem. Soc.*, 1958, **80**, 1339-1339.
- 22.X. Feng, X. Wang, W. Xing, B. Yu, L. Song and Y. Hu, *Ind. Eng. Chem. Res.*, 2013, **52**, 12906-12914.
- 23.B. Wang, Q. Tang, N. Hong, L. Song, L. Wang, Y. Shi and Y. Hu, *ACS Appl. Mater. Interfaces.*, 2011, **3**, 3754-3761.
- 24.D. Wang, L. Song, K. Zhou, X. Yu, Y. Hu and J. Wang, *J. Mater. Chem. A*, 2015, **3**, 14307-14317.
- 25.X. H. Li, Y. Z. Meng, Q. Zhu and S. C. Tjong, *Polym. Degrad. Stabil.*, 2003, **81**, 157-165.

**Table 1.** The data of cone calorimeter tests of neat EP and its composites.

| <b>Sample</b>      | <b>TTI (s)</b> | <b>PHRR<br/>(kW/m<sup>2</sup>)</b> | <b>THR<br/>(MJ/m<sup>2</sup>)</b> | <b>PSPR<br/>(m<sup>2</sup>/s)</b> | <b>FGI<br/>(kW/(m<sup>2</sup>·s))</b> |
|--------------------|----------------|------------------------------------|-----------------------------------|-----------------------------------|---------------------------------------|
| <b>EP</b>          | 65             | 1592                               | 77.5                              | 0.416                             | 17.3                                  |
| <b>MWCNT/EP</b>    | 70             | 1490                               | 75.4                              | 0.371                             | 16.0                                  |
| <b>G/EP</b>        | 76             | 1237                               | 67.6                              | 0.329                             | 12.4                                  |
| <b>MWCNT/2G/EP</b> | 71             | 1289                               | 67.0                              | 0.230                             | 13.0                                  |
| <b>MWCNT/G/EP</b>  | 75             | 1036                               | 58.1                              | 0.180                             | 10.6                                  |

## Figure Captions

**Scheme 1** Preparation path of MWCNT/G hybrid (a) and MWCNT/G/EP composite (b).

**Fig. 1** TEM images of G (a), MWCNT/2G hybrid (b), MWCNT/G hybrid (c); SEM image of MWCNT/G hybrid (d).

**Fig. 2** Typical FT-IR spectra of CS, GO, MWCNT, MWCNT, G, MWCNT/2G and MWCNT/G hybrid.

**Fig. 3** TGA curves of MWCNT, G, MWCNT/2G and MWCNT/G hybrid.

**Fig. 4** TGA/DTG profiles for EP and its composites as a function of temperature under air atmosphere.

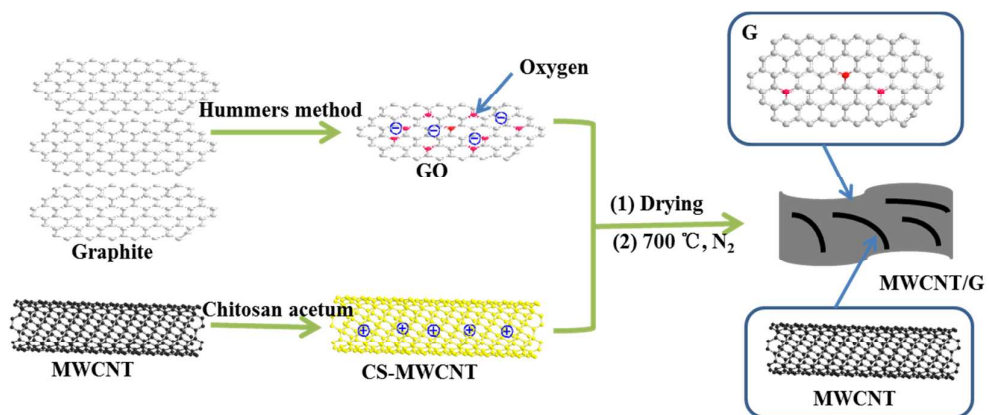
**Fig. 5** HRR curves of pure EP and its composites derived from MCC.

**Fig. 6** HRR and THR profiles of pure EP and its composites derived from cone calorimeter.

**Fig. 7** Absorbance of toxic gas for pure EP and MWCNT/G/EP composites: (a) total pyrolysis products (Gram-Schmidt), (b) hydrocarbons, (c) CO and (d) aromatic compounds.

**Fig. 8** SEM images of char residues for EP (a), MWNT/EP (b), G/EP (c), MWNT/2G/EP (d) and MWNT/G/EP (e).

**Fig. 9** Visual mechanism of the suppression of heat radiation and toxic effluent for MWCNT/EP (a), G/EP (b), MWCNT/2G/EP (c) and MWCNT/G/EP composites (d).



**Scheme 1** Self-assembly fabrication of MWCNT/G hybrid material by electrostatic attraction and thermal reduction.

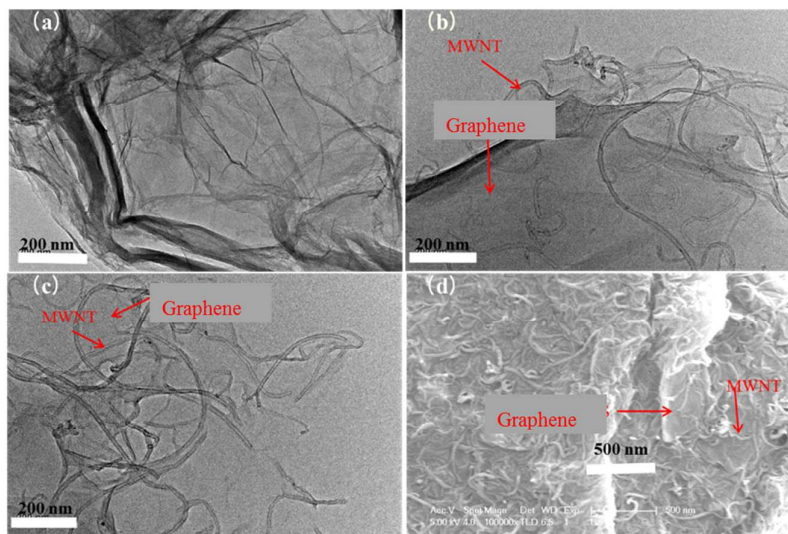


**Fig. 1** TEM images of graphene (a), MWCNT/2G (b) and MWCNT/G hybrid (c);

SEM of MWCNT/G hybrid (d).

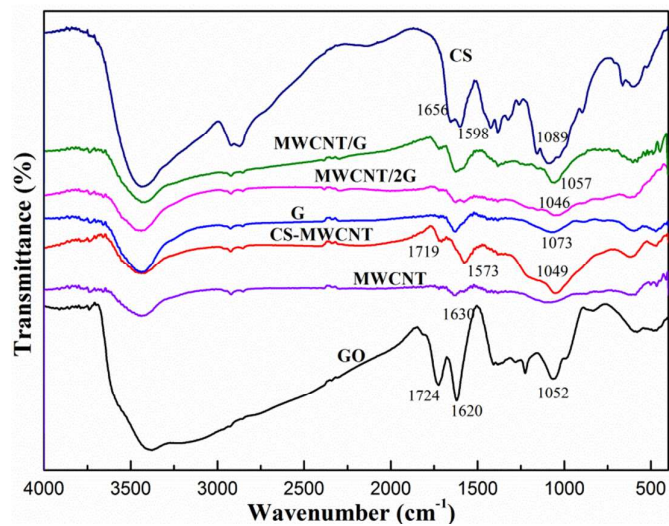


**Fig. 2** Typical FT-IR spectra of CS, GO, MWCNT, CS-MWCNT, G, MWCNT/2G and MWCNT/G hybrid material.

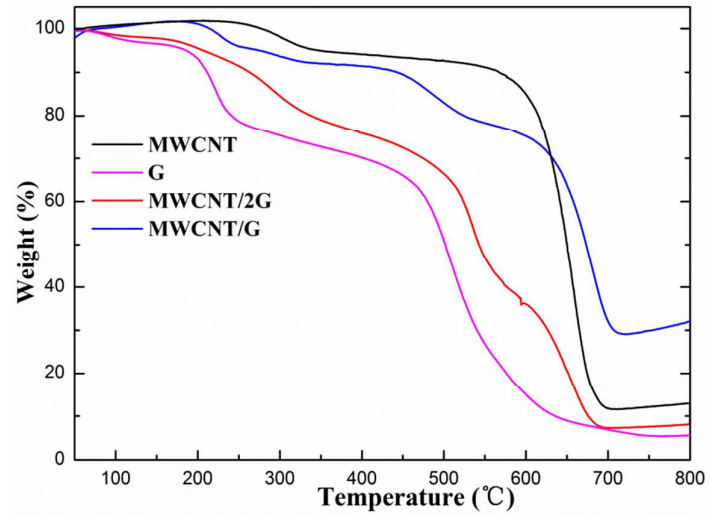


**Fig. 3** TGA curves of MWCNT, G, MWCNT/2G and MWCNT/G hybrid in air atmosphere

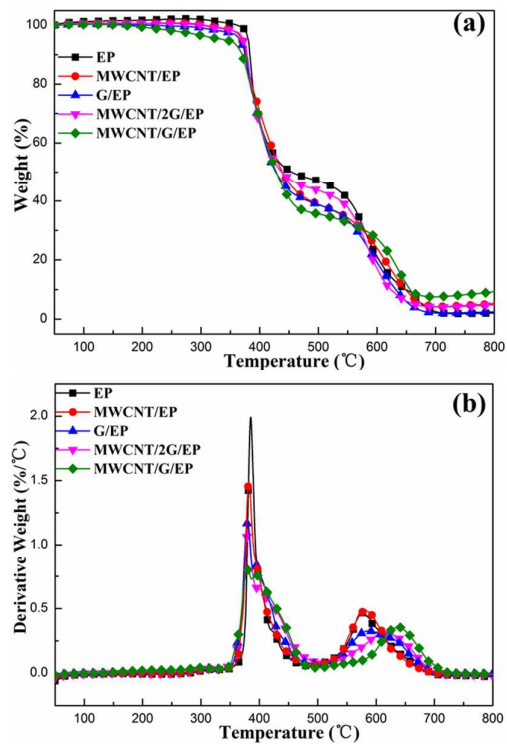


**Fig. 4** TGA/DTG profiles for EP and its composites as a function of temperature under air atmosphere.

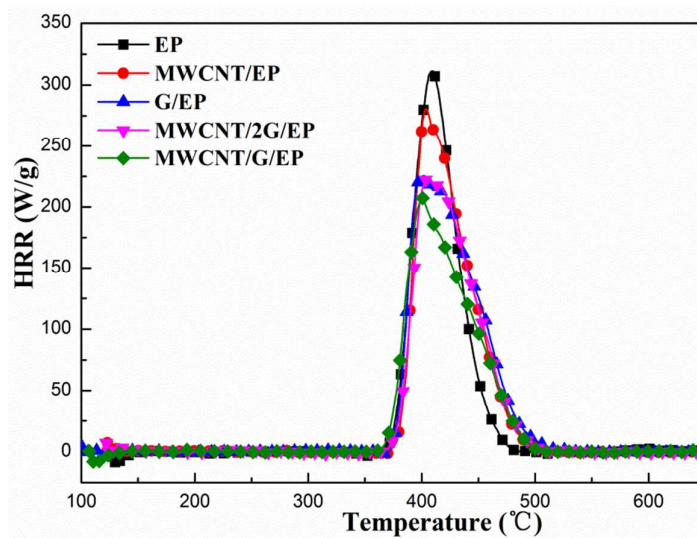


Fig. 5 HRR curves of neat EP and its composites derived from MCC.

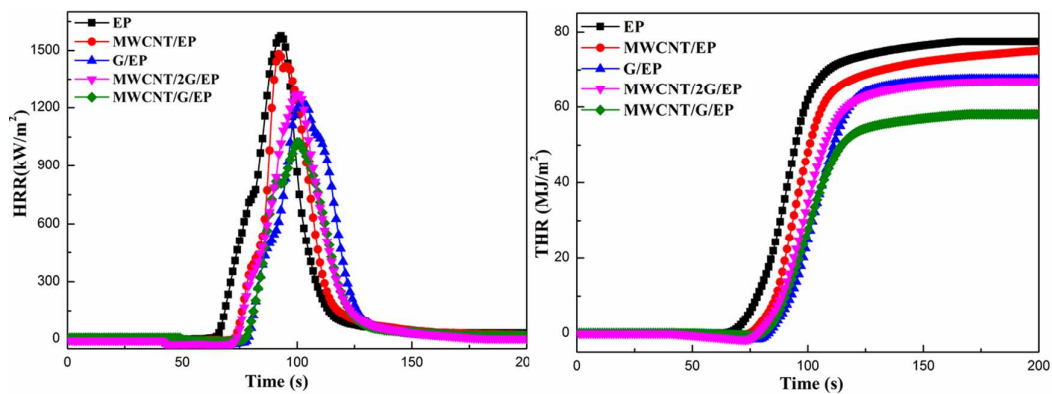
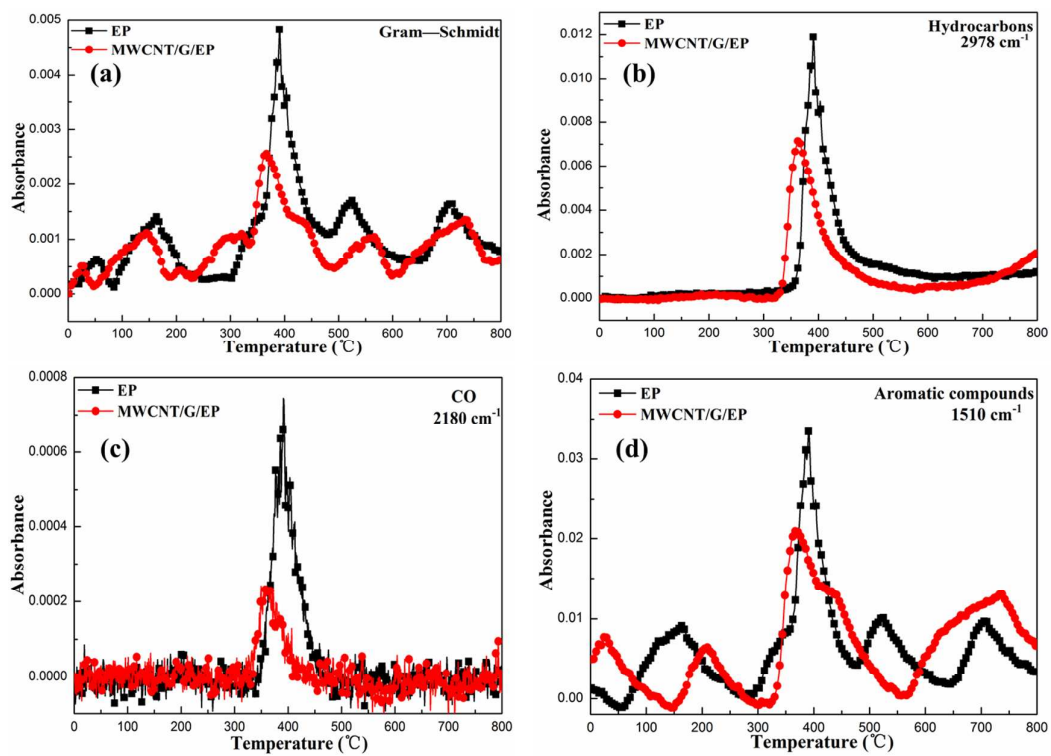
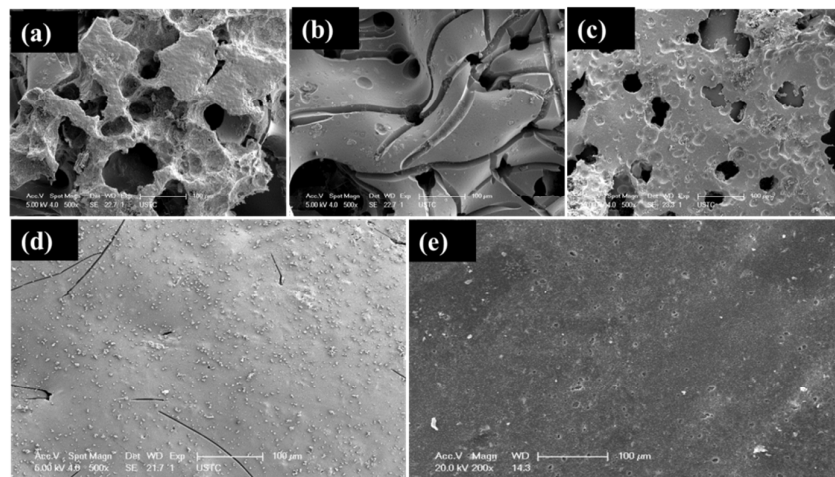


Fig. 6 HRR and THR profiles of neat EP and its composites derived from cone calorimeter.



**Fig. 7** Absorbance of toxic effluent for pure EP and MWCNT/G/EP composite: (a) total effluent (Gram-Schmidt), (b) hydrocarbons, (c) CO and (d) aromatic compounds.



**Fig. 8** SEM images of char residues for EP (a), MWCNT/EP (b), G/EP (c), MWCNT/2G/EP (d) and MWCNT/G/EP (e).

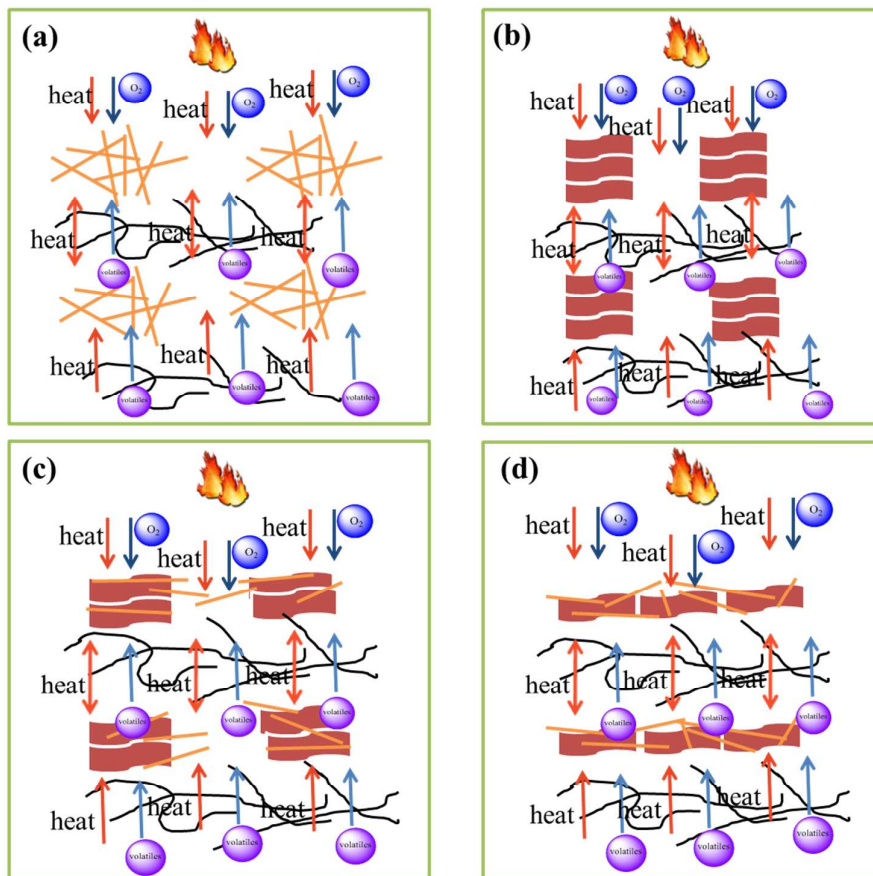


**Fig. 9** Visual suppression of heat radiation and toxic effluent of MWCNT/EP (a), G/EP (b), MWCNT/2G/EP (c) and MWCNT/G/EP composites (d).